Available online at www.sciencedirect.com
SCIENCE DIRECT
Catalysis Today 109 (2005) 185–194
CATALYSIS TODAY
www.elsevier.com/locate/cattod

Catalyst pore plugging effects on hydrocracking reactions in an Ebullated bed reactor operation

Roberto Galiasso Tailleur [1,*], Lino Caprioli

Simon Bolivar University, Department of Thermodynamics, Sartenejas, Baruta, Venezuela

Available online 3 October 2005

Abstract

This paper analyzes the deactivation effects of $NiMo/Al_2O_3$ catalyst during the operation in an Ebullated bed reactor for Heavy residue hydrocracking. The spent catalysts were characterized by chemical analysis, ^{13}C NMR, ESM, DRX, and by using thermal programmed oxidation and diffusion studies in a shallow bed micro-reactor. The deactivations were performed in a 5 l continuously stirred tank reactor, while the spent catalysts were tested in a 0.05 l micro-reactor. The study focused on determining the properties of the external layer of the catalyst and on evaluating the internal coke and metal deposition. The results indicated that initial deactivation is mainly due to coke depositions, while its impact on mass transfer reaction control depends on temperature. In long-term deactivation, the metal deposition plays a more important role in blocking the internal micro- and meso-structures and in building up the external layer of the pellets.

Keywords: Coke; Hydrocracking; Ebullated bed; Catalyst deactivation; Pore plugging; Effective diffusion

1. Introduction

Hydrocracking heavy oil in order to produce a more valuable product requires a high conversion to compensate the high capital investment needed to build this upgrading technology. As reported previously [1], upgrading economy is improved by working at a residue conversion higher than 70%. In an ''Ebullated bed'' reactor, the catalyst operates well when mixed at a high temperature (420–430 °C). However, it is quickly deactivated and needs to be continuously added and withdrawn. It is possible to treat high metal content feedstock using a high rate of catalyst replacement. In this case, catalyst consumption and disposal become an important part of the operating cost. Catalysts deactivation is caused by: (1) metal deposition on active catalytic surface and (2) the carbonaceous material deposition and precipitation on the external and internal structure of catalyst [2]. When the one-through fixed bed Hydrocracking conversion is increased above 50%, and depending on the characteristics of the crude considered, a ''mesophase'' is formed. This is a relatively insoluble material, which starts to precipitate on the catalytic surface conferring plugging problems that remain in suspension as fines particles. This phenomenon occurs because malthenes, the material that keeps the asphalthenic ''micelles'' soluble, crack faster than asphalthenes (Caprioli et al. [3], Higashi et al. [4]). In addition, the heavy molecules dealkylate and polymerize producing less soluble material than the original ones. To define the best operating temperature (and conversion) it is important to study the impact of catalyst deactivation in pore diffusion. There are many studies in the literature [5–8] that analyze the metal distribution along the pore radius for fixed bed operations, but few studies analyze Ebullated bed reactors [9,10]. Woof and Gladden [11], among others, discuss the effect of coke deposition on self-diffusion in deactivated hydroprocessing catalysts.

The aim of the present experimental work is to demonstrate the effect of the catalyst external layer on mass transfer and on the reactions that take place in an Ebullated bed reactor for heavy residue hydrocracking at medium conversion.

2. Experimental

Four types of activities have been performed:

* Corresponding author. Tel.: +34 963690668.
E-mail address: Gatairo@itq.upv.es (R. Galiasso Tailleur).
[1] Retired from PDVSA Intevep in 2005.

0920-5861/$ – see front matter © 2005 Elsevier B.V. All rights reserved.
doi:10.1016/j.cattod.2005.08.026

(1) Catalyst characterization and effective diffusivity measurements.
(2) Pilot plant catalyst deactivation in a CSTR.
(3) Micro-plant activity test of spent catalyst in pellet and in powder.
(4) Micro-plant activity test of spent scratched and regenerated pellets.

2.1. Catalyst characterization

The proprietary $NiMo/Al_2O_3$ catalyst used was characterized after one week on stream, operating at three temperatures. The solids produced at 410, 420 and 430 °C were called D1, D2, and D3, respectively. Other samples of catalyst were also operated continuously for six months at 410 °C, and for three months at 430 °C, producing the samples named D4 and D5. After that, all solids were washed with toluene at 80 °C during 4 h, dried at 120 °C in nitrogen, and extracted with CS_2 at 60 °C. The extracts obtained were concentrated and analyzed. The catalyst was dried again and divided into three portions which were called: (1) pellets, (2) scratched pellets (s-pellets), and (3) ground pellets (p-pellets), which are the size of less than a 150 μm average particle. The s-pellets were obtained from selected equal-size pellets by manually removing the external layer (one-by-one), using a plastic device to support the pellet and a scalp. The powder resulting from the scratching of 20 pellets with the same deactivation was blended and characterized (s-powder).

2.1.1. Textural properties

Surface, pore volume, and pore diameter were measured using standard nitrogen adsorption–desorption methods, adapted for pellet measurements. The results were reported (Table 1) and defined as micro-pore – referring to the volume in the region between 0 and 2 nm of pore diameter – and as meso-pore, for the region from 2 to 50 nm. The three N_2 adsorption–desorption measurements (micro-meritics equipment) as function of relative partial pressure were done with five different pellet samples (obtained at the same deactivation conditions) to verify the hysterisis phenomenon and reported as an average plot in Fig. 1. The macro-porous volume is defined as total pore volume minus the micro- and meso-pore volume.

Table 1
Catalyst properties

Properties	Initial	D1	D2	D3	D4	D5
MoO_3 (wt%)				12.5		
NiO (wt%)	4.2	4.7	4.6	4.7	12.3	9.4
V (wt%)	0	3.7	3.7	3.8	60.48	40.32
Macro-pore volume (cm^3/g)	0.19	0.16	0.15	0.15	0.09	0.06
Meso-pore volume (cm^3/g)	0.25	0.21	0.19	0.17	0.09	0.11
Micro-pore volume (cm^3/g)	0.15	0.08	0.03	0.01	0	0
C/H	–	0.9	0.88	0.84	0.96	0.94
Soluble in xylene (wt%)	–	0.6	0.45	0.3	0.4	0.45
Carbon (wt%) pellet	–	6.1	6.4	7.1	8.9	9.8
Carbon (wt%) scratched pellet		5.3	5.4	5.6	6.1	5.9
Sulfur (wt%)	5.8	6.32	6.44	6.55	10.4	10.1
C_5/He effective diffusion (cm^2/seg)	0.08	0.0065	0.0033	0.0028	0.0021	–

2.1.2. SEM

The scanning electron microscopy was performed using ISI-70 apparatus and the radial profile of coke and vanadium was measured using an EDAX system at 30 kV (1000 msg accumulation). The electron back-scattering (EBS) microphotography and point-by-point microanalysis of the dispersion energies (500 mgs in point by point analysis) were also carried out. The pellets were imbedded in plastic, cut cross over the particle diameter to expose the inner transversal surface, and covered with a thin film of gold using electro-deposition to improve their conductivity (Fig. 2). EDAX analysis was also made along the external particle diameter (flat face-gold covered (Figs. 3 and 4). Particular care was taken to avoid transferring coke from one zone to another. The system was calibrated using fresh catalyst containing artificially deposited

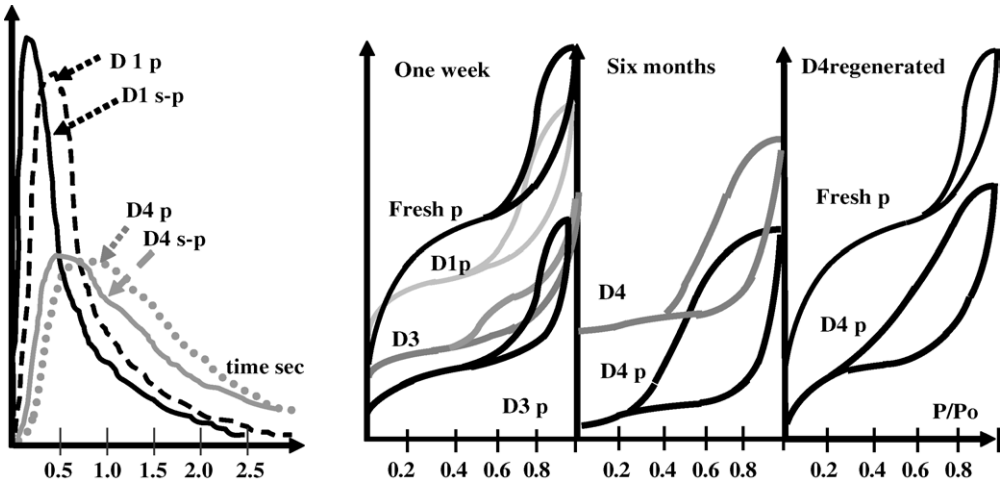

Fig. 1. C5 pulse output signal (left) and nitrogen sorption measurements (right).

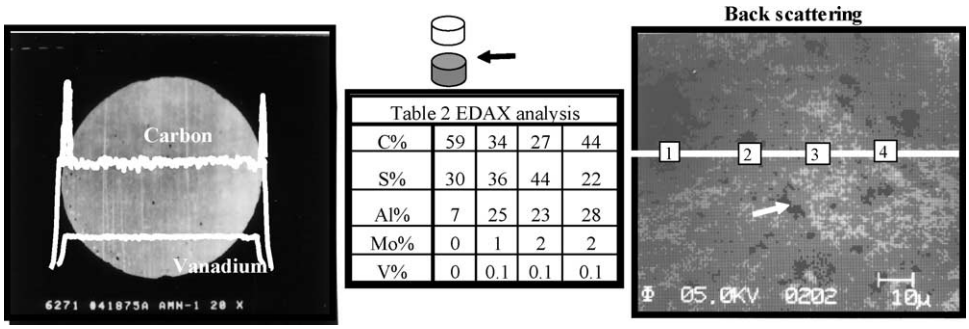

Table 2 EDAX analysis

C%	59	34	27	44
S%	30	36	44	22
Al%	7	25	23	28
Mo%	0	1	2	2
V%	0	0.1	0.1	0.1

Fig. 2. EDAX (left), four points analysis (center), and EBS microphotography (right).

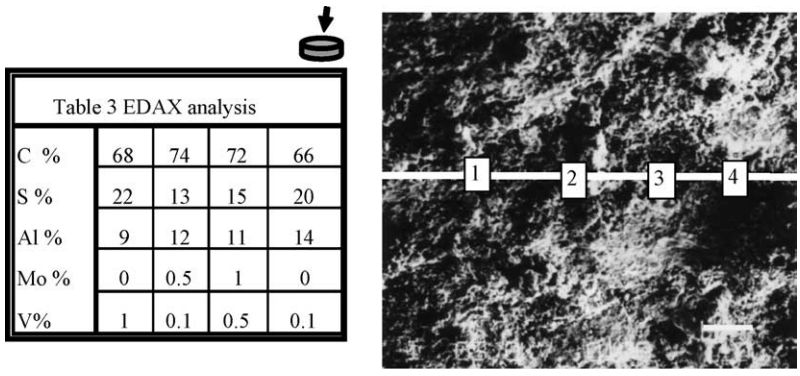

Table 3 EDAX analysis

C %	68	74	72	66
S %	22	13	15	20
Al %	9	12	11	14
Mo %	0	0.5	1	0
V%	1	0.1	0.5	0.1

Fig. 3. Four point analysis and EBS microphotography.

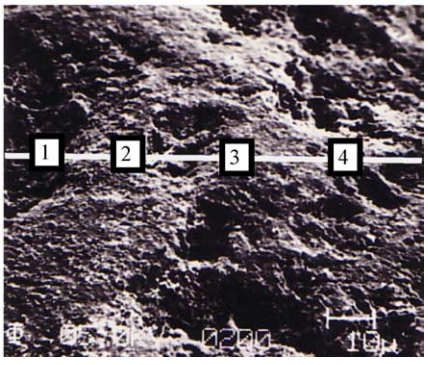

Table 4 EDAX analysis

C%	28	34	27	22
S%	34	28	32	40
Al%	3	0	1	1
Mo%	0.1	0.1	0.1	0.1
V%	35	38	40	37

Fig. 4. Four point analysis and EBS microphotography.

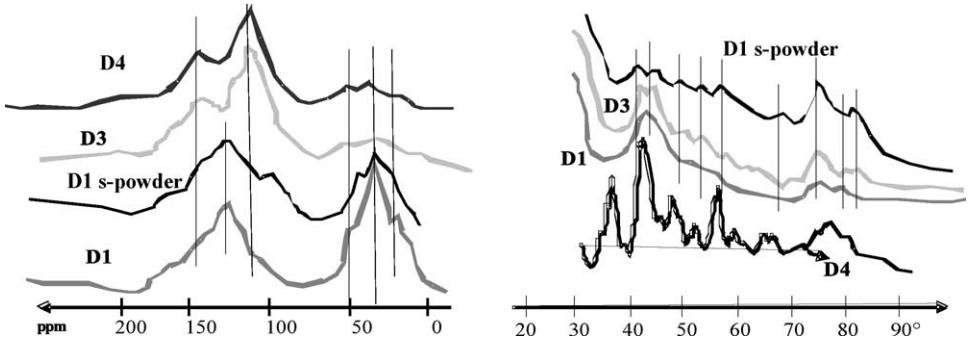

Fig. 5. ^{13}C NMR (left) DRX (right) analysis of D1, D2, D3, D4 pellets and D1 s-powder.

coke (from cyclo-pentane) and vanadium (from vanadyl porphyrin).

2.1.3. Solid ^{13}C NMR spectra

The spectra were performed using a Varian spectrometer operating at a frequency of 100.58 MHz with cross-polarization to detect the type of carbon present in the sample (Fig. 5, left side). The internal reference used was trimethylsilyl. The spectra were interpreted based on Callejas et al. results [12].

2.1.4. XRD

Difractograms were taken in a Philips 1812 at 45 V and 30 mA with data acquisition, registered continuously from 5 to 95° at 0.015° 2θ/s rate. The weak signals attributed to γ-alumina were measured, accumulated in the computer and discounted in all difractrograms with the hypothesis that are still present in the deactivated sample. The spectra only contain the graphite signals indicated (Fig. 5, right side) with vertical lines.

2.1.5. Effective diffusion measurements

A shallow bed reactor (Fig. 6, right side) was employed to measure the effective diffusivity with C_5 on Helium gases using the methodology developed by Sun et al. [13]. The 21 pellets with the same deactivation were installed in a flat layer and the He flow rates were established. The samples were heated at 100 °C in helium and maintained under this condition for 24 h; then 10 successive pulses of pentane were injected at the inlet of the shallow bed and, simultaneously, 10 others of helium were injected at the outlet. That was done at the outlet in order to keep equal pressure on both sides of the particle. The C_5 concentration at the output was measured by conductimetry as a function of time (see raw peaks in Fig. 1, left side). The values of effective diffusivity were calculated after computerized deduction of back-mixing and dead volume reported in Table 1. These two effects were previously calculated by ''blank'' experiments performed on micro-porous and a meso-porous alumina at different He flow rates and C_5 pulse sizes. The procedure and the equations needed to obtain the effective diffusion coefficient from the first and second momentum from the transient response to a C_5 tracer impulse input will be elsewhere [14]. Negligible C_5 adsorption was measured with all deactivated catalysts. Other details about the technique can be seen in Paerk et al. [15].

2.1.6. TPO

The thermal programmed oxidation of spent catalysts was conducted in a shallow bed reactor (21 particles; Fig. 6, right side) where the solid was heated (10 °C/min) in presence of 2% of oxygen in nitrogen gas mixture at a flow rate of 50 ml/min. The CO_2 and other gases formed were monitored by a calibrated GC method. A TPO analysis of 20 commercial pellets of spent HDS catalyst ($NiMo/Al_2O_3$) that treated VGO during 18 months, containing 9% of coke and well distributed along the diameter, was also made as reference (Ref).

2.1.7. Metals determination

Analysis of metals was performed by atomic adsorption spectroscopy (Varian Techtron analyzer). Metals were reported in percent by weight (bulk) of total metal in the support (Ni, Mo, C, H, V, and S/support) (see Table 1).

2.2. Pilot plant operation

2.2.1. Feed

The feed was vacuum residue from Jobo-Morichal crude of the Orinoco Belt in Venezuela. It has an initial boiling point of 490 °C, and contains 5.02% of sulfur, 0.93% of nitrogen, 22% of carbon Conradson, 21 wt% of *n*-C7, 32.05 wt% of *n*-C5 insoluble asphalthenes, and 714 wtppm of vanadium (Table 5, standard ASTM methods of analysis). Other important properties like C–H and aromatics in coke on catalyst and in insoluble material were determined by solid ^{13}C RMN analysis. The Hot Filtration Test (HFT-ASTM WK783) was used to measure the micro-coke formed in the products.

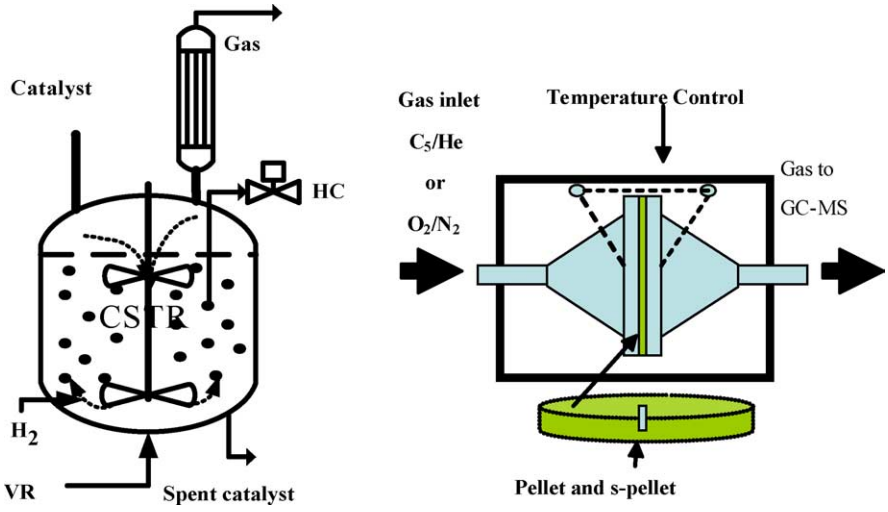

Fig. 6. Continuous stirred tank reactor (left) and shallow bed reactor (right).

2.2.2. CSTR

To evaluate the reactivity, two different sets of deactivation experiments were carried out at the 5 l continuously stirred tank reactor (CSTR) pilot plant. This simulates an Ebullated bed reactor operation. The details about the plant can be seen in reference [16] and those about the reactor can be seen in Fig. 6 (left side).

1. The first set of experiments was dedicated to produce three samples of catalyst deactivated at different temperatures. The three CSTR tests were operated for one week at 23.6 MPa, and H_2/HC ratio of 10 (molar), but the temperatures were 410, 420, and 430 °C with space velocity of 0.5, 0.66, and 0.91 h^{-1}, respectively, to keep 50 wt% of 500 °C conversion (HCK). The catalyst was installed in the reactor and presulfided using a hydrogen and diesel spike with 0.1% of CS_2, at 300 °C for 6 h. Then the vacuum residue was fed to the reactor and operated without adding or withdrawing catalyst to have all the particles with the same age. Then, after one week, the unit was shutdown and the catalyst were removed, washed, dried, and characterized (D1, D2, and D3 in Table 1).
2. The second set of experiments was carried out at 410 and 430 °C (the other conditions were similar to the previous one) with the same catalyst, operating continuously for six and three months, respectively, without adding or withdrawing catalyst (D4 and D5).

All catalyst samples (pellets, s-pellet and p-pellet) were tested in the 0.05 l reactor to determine the activity of the spent and regenerated catalyst. The operating conditions were 410 °C, 25.6 MPa, and different space velocity to have around the same HCK conversion.

3. Results

3.1. Catalysts deactivated by coke at three temperatures

The properties of used catalysts are shown in Table 1. Metal content is reported by weight of regenerated sample, whereas carbon is reported by weight of xylene washed and dried catalyst. After a one week operation at 410 °C all the reactions are decreased, and spent catalyst (D1) contains 6.1 wt% of coke with a carbon/hydrogen ratio of 0.9 (wt). The volumes of micro- and meso-pore regions are 0.21 and 0.08 cm^3/g, which shows an important reduction with respect to the initial catalyst values (0.25 and 0.15 cm^3/g, respectively). The macro-pores volume seems less changed. At this time on stream, vanadium concentration on catalyst (VOC) is around 3.7%, and the additional Ni is 0.5 wt%. Fig. 2 shows the SEM analysis for the middle of the pellets. The cross sectional D1 EDAX analysis depicts a sharp peak of carbon content in the border of the particle and an oscillating ''uniform'' flat carbon and vanadium profiles along the particle diameter (left side). Back scattering (EBS) electron microphotography – right side of the figure – indicates the presence of carbon patches well distributed along the radius, and the EDAX analysis (200 point-by-point measures) confirms the micro-heterogeneity of the carbon on the inner part (see, for example, the four points composition in Table 2; Fig. 2).

Table 2
Four points EDAX analysis (Fig. 2)

	Points			
	1	2	3	4
C (%)	59	34	27	44
S (%)	30	36	44	22
Al (%)	7	25	23	28
Mo (%)	0	1	2	2
V (%)	0	0.1	0.1	0.1

The internal carbon deposition seems to depend on the concentration of the cracking reaction intermediaries, and the flat profile along the particle diameter for both vanadium and coke indicate that the reactions, which generated the initial macroscopic deposition, are not limited by pore diffusion of reactant at this temperature. The ^{13}C RMN peaks at 15 ppm (Fig. 5, left side) indicated that coke on pellet was mainly composed of aromatic polymers [12]. DRX analysis depicted in Fig. 5 (right side), D1 curve, where vertical lines correspond to graphite structure (JCPDS 13-0148), confirms the minor presence of crystalline carbon deposits (signals of alumina were subtracted from the spectra (JCPDS 4-877).

The external layer of coke is formed by adsorption of some carbonaceous material (resins–asphalthenes) on the outer pellet surface, including the mouth of pores. This layer is not removed by toluene washing, and it is well attached to the catalyst. It is important to remember that in Ebullated bed operation, catalyst particles are shaken and washed by continuous impacts of liquid and bubbles, resulting in lower probability of micro-coke sticking than in fixed bed operation. The amount of coke in the remaining s-pellets is now 5.8%, and the difference between pellets and s-pellets is due to the coke in the external layer. The s-pellets micro- and macro-pore volumes are quite the same than those measured in pellets. In other words, the volume of the pores is unaffected by the scratching. EBS microphotography of the external flat part of the pellet (Fig. 3, right side) shows a lower micro-heterogeneity (dark spot signaled by arrow) in comparison with the internal one. EDAX analysis of the external layer (the composition of four isolated points are shown in Table 3; Fig. 3) confirms the presence of a porous carbon-predominant layer. This agrees with the chemical analysis of the s-powder obtained from 21 D1 pellets (65 wt% carbon, 20 wt% sulfur 14 wt% alumina, and 1 wt% vanadium). The ^{13}C NMR analysis of the s-powder (Fig. 5, left side, D1 s-powder) confirms the presence of a less aromatic polymer (peak at 40 ppm) than in D1 pellets, and the presence of pre-graphitic type material (peak at 138 ppm [12]). The DRX analysis (Fig. 5, right side, D1 s-powder) pointed out the presence of a better-defined graphite type structure.

The other two catalysts deactivated at a higher temperature (D2 and D3) have more or less the same amount of vanadium, but 2 and 5%, respectively, of additional coke content than D1. The amount of xylene insoluble material is increased, C/H ratio

Table 3
Four points EDAX analysis (Fig. 3)

	Points			
	1	2	3	4
C (%)	68	74	72	66
S (%)	22	13	15	20
Al (%)	9	12	11	14
Mo (%)	0	0.5	1	0
V (%)	1	0.1	0.5	0.1

is slightly reduced, and the volume of micro-pore is decreased to very low values with the rise in deactivation temperature. The SEM analysis (not shown) for D2 and D3 pellets depicts a similar internal ''flat'' profile of coke with the same micro-heterogeneity (patches), as well as a similar external carbonaceous layer of coke to those of D1. Nevertheless, the deactivation temperature affects vanadium profile along the particle diameter, which shows an incipient U-type profile (well described in the literature for fixed bed HDM operation [8]) suggesting the existence of a diffusion control of HDM reaction. The D3 ^{13}C NMR analysis of the pellets indicates the same two broad bands than D1, associated to aromatic polymers (40 ppm) and pre-graphite structure (138 ppm), but D3 DRX spectrum presents a higher crystalline DRX coke signal (graphite). The D3 s-powder chemical analysis confirms a high contribution of carbon in the external layer (82% C, 12% S, and 6% Al) and a similar DRX spectrum to the D1 layer. The concentrations of V and C in D2 and D3 s-pellets are quite similar to those of D1 s-pellets, but the difference between pellets and s-pellets increased when deactivation temperature increased as a result of the coke found in the external layer. The higher the operating temperature, the higher is the thermal cracking reaction and the product adsorption on surface (see in Table 5; HFT, how the micro-coke is augmented). Further on, we will analyze the permeability of this external layer and the activity of the catalyst.

3.2. Catalysts deactivated by vanadium and coke

The long-term deactivated catalysts (D4 and D5) are completely different to those at start-of-run, described above. The amount of vanadium and nickel deposited on the surface are 60 and 8.55 wt%, respectively, for D4. The difference between carbon in six-month pellets and that in one-week pellets is 44%, although the difference for the s-pellets is only 18% higher. This means that a small amount of additional coke is deposited during the cycle in the internal pore structure, and most of the coke is built up in the external layer. The longer the time on stream, the lower is the meso-pores volume (being negligibly the micro-pore volume), the hydrogen content in the coke, and the xylene-soluble material. The SEM analysis of D4 pellets (not shown) presents the typical U-shape type profile across the particle diameter for vanadium, sulfur, and Ni, agreeing with results observed previously for the same catalyst in fixed bed [7], as well as by other authors [8,17,18]. But D4 also has an acute U-shape profile for carbon, already seen in commercially operated Ebullated bed hydrocracker plants [14]. The difference here is the presence of this thin external layer containing most of the coke, some vanadium, and sulfur. For example, the D4 s-powder contains 65% of coke, 15% of vanadium, and 20% of sulfur. EBS microphotography of internal coke (not shown) indicated a lower internal micro-heterogeneity than D1, and the 200 point-by-point EDAX analysis suggested the presence of large clusters of vanadium and sulfur on surface with some coke in it. The external particle microphotography (D4, Fig. 4, left side) presents less heterogeneity and a probably lower porosity than D1, and shows that vanadium and sulfur concentrations dominate in the clusters (Table 4 in Fig. 4), agreeing with the high vanadium content of the sample.

The ^{13}C NMR analysis (D4 pellet in Fig. 5, left side) presents a different types of signal in the range of 130 and 150 ppm attributed to a distorted graphite type structure and another one due to a different type of polymeric coke, being the latter similar to those shown in the D3 sample. DRX spectra (D4, Fig. 5, right side) show a strong crystalline signal attributed to some low sulfided V and Ni Fe species, plus a graphite superimposed signal. The chemical analysis (S/V ratio) might support this idea but the DRX computerized interpretation of the spectra is affected by the potential contribution of some aluminium–vanadium crystalline compound not considered and by the heterogeneity of the cluster, giving no bases for further analysis. Other authors indicated the presence of highly sulfided V species [19,20] on their catalysts. The ^{13}C NMR and DRX of the D4 s-powder are similar to those of D4 pellets.

Sample D5 was obtained after three months on stream at 430 °C, but at a lower residence time than D4. The operation was shut down because the activity of the catalyst was too low for the hydrocracking reaction. D5 pellets contain higher amounts of coke than D4 pellets, while D5 s-pellets contain less than D4 s-pellets samples. The main difference is in the external layer, which is built up by operating at a higher temperature. The D5 internal U-profile concentrations for all of the components on the surface (C, S, Ni and C) of the pellet cross section (EDAX analysis) are more pronounced than in D4, indicating a stronger mass transfer control in the outer part of the pellets for all the reactions. The external layer is now composed by 50% C, 43% V, and 17% S, and is quite homogeneous in its composition, presenting a similar highly crystalline graphite – plus some indication of the presence of vanadium crystalline sulfides (^{13}C NMR; DRX-JCPDS 29-1382/36-1132) – to those observed in D4 layer (Fig. 5). The permeability of this layer will be discussed below.

Table 4
Four points EDAX analysis (Fig. 4)

	Points			
	1	2	3	4
C (%)	28	34	27	22
S (%)	34	28	32	40
Al (%)	3	0	1	1
Mo (%)	0.1	0.1	0.1	0.1
V (%)	35	38	40	37

3.3. Measure of diffusion coefficient

The 20 pellets installed in the shallow bed reactor were used to determine the C5 diffusion coefficient of deactivated catalyst (Table 1). The effective diffusion coefficient for the non-adsorbed C_5 hydrocarbon tracer in helium is calculated using the methodology described elsewhere [14]. Typical raw output is represented in Fig. 1, left side, where four curves can be seen. Two of them correspond to D1, pellets and s-pellets, and the other two to D4, pellets and s-pellets. The signals are composed by a main Gaussian-type shape followed by a long tail (for fresh catalyst only have Gaussian curves). When no tracer adsorption is present (verified with fresh catalyst steady state adsorption and desorption measurement), the first one is associated to the presence of a meso-structure (molecular diffusion) and the tail is associated to the micro-pores (Knudsen diffusion) and bottleneck meso- and macro-pore that retard the output information (tail). The "blank" measurement provided information about the momentum associated to gas dispersion and dead volume in the shallow bed reactor, which are deducted from the raw curve depicted in Fig. 1, to calculate the effective diffusion (Gaussian part of the curve). It can be seen that, for both catalysts, eliminating the external layer improves the C_5 effective diffusion coefficient. In D1, the outer film reduces the diffusivity but slightly affects the tail, indicating that this external layer might be meso-porous and is still permeable to C_5. Table 1 indicated that the higher the short-term deactivation temperature, the lower the effective diffusivity and the larger the tail that might point to the reduction in the external layer permeability. For long-term deactivation at 410 °C the D4 pellets curve indicated a very low diffusivity with a longer tail. Now the effect of eliminating the external layer is less noticeable than in the previous one. The external part of the pellets, where coke and vanadium are concentrated, has lost most of its permeability, and the long tail is assigned to dead-end bottle-type pores. Here, the mouth of meso-pores is being narrowed by coke and metal depositions and a smaller mouth was created to connect macro and meso-structures.

The presence of dead-end pores has been verified by the hysterisis in nitrogen adsorption–desorption studies in deactivated pellets and s-pellets of catalyst. The left side of Fig. 1 shows the difference in the hysterisis for D1 pellets and D3 pellets (notice that the *Y* axis scale is only for fresh D3p, D4p an D4pr catalysts, the other being moved up). The higher the temperature, the larger is the hysterisis, but when D3 pellets are scratched this phenomenon is quite similar for both catalysts (compare D3 s–p with D1 s–p). The highest hysterisis (Fig. 1) during N2 desorption occurred for D4 pellets catalyst, but after removing its external layer (D4 s–p) the hysterisis was slightly reduced. Finally, in regenerated D4 sample (D4r) – see right side of Fig. 1 – there is a strong N_2 hysterisis, which, although diminished by the carbon removal during oxidation, is still much higher than those observed in fresh or in D1 catalysts. The regenerated D4 catalyst has 0.13 and 0.05 cm^3/g of meso- and micro-porosity, indicating some pore volume recovery.

Due to the high external pore blocking it was not possible to measure the C_5 diffusion coefficient, nor to perform a reliable N_2 adsorption study on D5 pellet or s-pellets.

In both experiments, N_2 hysterisis and the tail in C_5 diffusion measurement point out the role of metals and carbon in changing the tortuosity factor in the periodically constricted pore structure, and in introducing a severe pore mouth plugging. The external layer introduces an additional resistance to the reactive and product diffusion.

3.4. TPO analysis

The oxidation of the carbon on surface was made using a ramp of temperature in the sallow bed reactor. The literature [20,21] for TPO of HDS catalyst in powder established clearly the presence of two main peaks for start-of-run periods, due to two species of coke. The first peak at 250–300 °C corresponds to an easy burning coke, due to its high hydrogen content and good accessibility. It is supposed to be placed on top of, or near to metals, and well distributed. Another peak appears later at 350–500 °C and is associated to other highly graphitic coke, structured on the alumina support.

The 21 pellets of spent catalyst placed in the shallow bed reactor were treated with oxygen using a ramp of temperature, and CO_2, SO_2, CO, and NO were measured. Fig. 7, left side shows the plot of CO_2 as a function of time. The three upper curves correspond to D1, D2, and D3 in pellet, the one in the

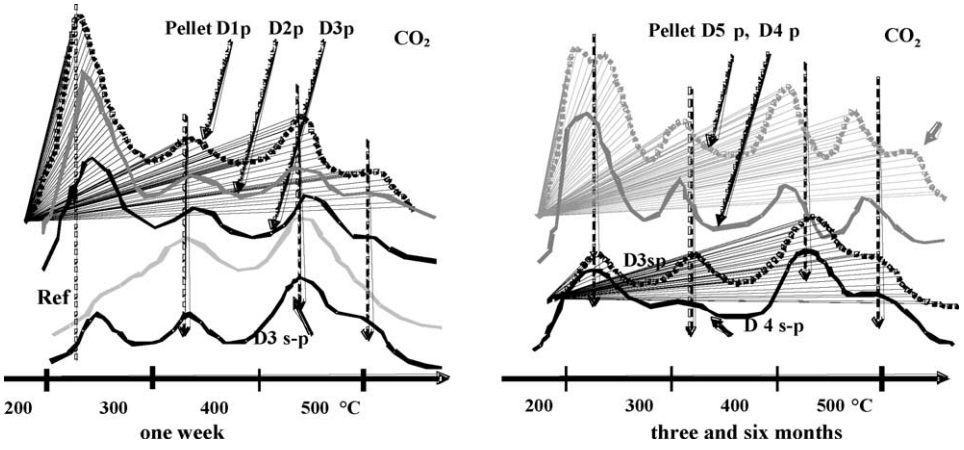

Fig. 7. TPO for short-term (left) and long-term (right) deactivation samples.

middle to D1 s-pellets and the lower one to REF catalyst. One can immediately notice the difference in the burning behavior between REF catalyst – in agreement with previous published information carried out with powdered catalyst – and all the residue-deactivated catalysts, which have four peaks. In D1, D2, and D3 TPO, there is a first peak (~230 °C) that moved up by increasing the deactivation temperature (from D1 to D3) and by removing the external layer D3 s-pellets. At the same time 40% sulfur, 90% hydrogen, and 8% nitrogen (not shown) are also burned. Then the second peak that appears at a higher temperature (320 °C) is similar to those reported by other authors and is assigned to internally easy-to-burn coke, placed near the outer part of the particle and on top of or near the metals sites. The third peak occurred around 435 °C and is only due to carbon burning. It is associated to a multi-layer of graphite type carbon, located in large (accessible) pores. The last one appears at higher burning temperatures and at the same time SO_2 and NO_2 are produced. The last signal of coke burning (503 °C) is probably due to coke in the small pores or bottle type pores where the oxygen access might be blocked or hindered. The s-pellets in which the external layer was partially removed show a smaller first peak of CO_2 and similar other ones. The second and third SO_2 peaks for D_1, D_2, and D_3 (attributed here to sulfur in metals and carbon present in the internal pore structure) are quite similar to those measured for s-pellets. In these samples, there are still low contributions of sulfur from vanadium. All information regarding CO_2 and SO_2 was confirmed with D1 and D2 s-pellets by using different rates of temperature increase (to measure the rate of carbon and sulfur oxidation) in the TPO, and by burning an artificially deposited uniform coke profile on the fresh catalyst. The TPO of D3 sample, and the more graphitic (less hydrogen content) and less permeably carbonaceous characteristics in the external layer of the pellets have shown the lowest rate of coke and sulfur burning at low temperature.

The oxidation of coke (TPO) in the long-term deactivated D4 pellets (Fig. 7, right side) presents similar peaks to the previous one, but with different intensity. The initial burning off occurs at a little lower temperature than those deposited at the start-of-run, probably catalyzed by the large amount of vanadium present in its external layer. But now the elimination of the external layer (delayering) produces lower first peaks for CO_2 and SO_2 due to the large amount of vanadium and coke near the outer border of the s-pellet (which gave place to a U-shape distribution across the pellet diameter). The accumulation of metal and sulfur also limits the access of oxygen into the meso- and micro-pore structure during the burning. By changing the rate of heating in the TPO, the shapes of peaks changed more in D4 pellets than in s-pellets. Carbon and sulfur in s-pellets – those that are early oxidized – are probably located in meso- and macro-pores where high amounts of vanadium might be stored. The D4 s-pellets sample presents the same peaks than D1 s-pellets, though with slightly higher coke burning and higher sulfur oxidations rates, agreeing with their higher contribution of vanadium and similar coke contents. TPO for D5p sample provided quite the same information than D4p, though it presents a fifth peak (see the arrow at 550 °C) attributed to a low accessible coke.

Table 5
Effect of temperature on VR properties

Properties	Feed	Temperature (°C)		
		410	420	430
Yield (wt%)	100	50.3	50.2	50.8
Density (g/cm)	1.091	1.031	1.019	1.005
Nitrogen (wt%)	0.903	0.925	1.13	1.32
Sulfur (wt%)	5.02	2.34	2.44	2.55
Carbon Conradson (wt%)	22	19	21	24
C7 asphalthenes (wt%)	21	24.3	26.3	27.5
C5–C7 asphalthenes (wt%)	14	8	9.1	10.2
Vanadium (wt ppm)	739	700	900	1050
Nickel (wt ppm)	98	45	50	61
Insoluble (HFT) (wt%)	0	0	0.01	0.05
Molecular weight (GPC)	1250	1080	1000	970

3.5. Catalyst activity

3.5.1. Effects of temperature in conversion with fresh catalyst

Catalytic activities are measured for fresh catalysts at three temperatures (410, 420, and 430 °C) but using different space velocity to obtain 50% of Hydrocracking (HCK) conversion. Hydrodesulfurization (HDS) and hydrodemetallation (HDM) reactions are evaluated. Table 5 presents the analysis of the feed and the vacuum residue products after reaction. At 410 °C and with fresh catalyst, 81% of HDM, 77% of HDS, 60% of CCR, and 53% of asphalthene removal were measured. At higher temperature the selectivity changes due to the effect of different activation energies [3] for the reactions involved. By rising the temperature, sulfur, nitrogen, metals, aromatics, asphalthene, and carbon Conradson increase in the unconverted VR, while the average molecular weight decreases. The presence of insoluble material (HFT) in high temperature products must be noticed. The insoluble material was composed of 87% C, 0.5%

Table 6
Product distribution for three deactivation temperatures

Product (wt%)	Properties											
	Yields			Sulfur			Nitrogen			Aromatics		
Gas	3.5	4	4.5	0.03	0.04	0.05	0.005	0.006	0.007	0	0	0
Naphtha	10	11	12	0.5	0.55	0.6	0.0045	0.005	0.006	10	13	17
Diesel	14	15	15.5	1.3	1.15	1	0.34	0.37	0.41	18	21	23
VGO	22.5	20	18	1.7	1.6	1.5	0.67	0.73	0.77	25	22.5	20.1

N, 8% S, 3% V, 1% Al with a poly-aromatics structure similar to the asphalthenes. The yield and quality of the product (Table 6) indicate that the higher the temperature, the higher the production of light materials and the concentration of contaminants (S, N, Aromatics) in the product. The product composition was changed at the same conversion as a consequence of different temperature effects on cracking and hydrogenation reactions (Caprioli et al. [16]).

3.5.2. Effects of temperature on catalysts on stream during one week

After one week operating at a constant temperature and HCK conversions with VR, the activity of the catalyst was still close to the initial ones. Table 7 presents, in the upper part, the value of the activities, and in the lower part, the selectivity ratio for catalyst in pellet and in powder, measured at 410 °C and 50% HCK conversion. It must be noticed that HDS and HDM conversions (rate of reactions) and the selectivity HDS/HDM are always higher for the powder than for the pellet, in agreement with previous findings about the mass transfer control of reactions [8,9,16].

Now, by comparing D1, D2, and D3 samples with fresh catalyst at similar HCK conversion, a strong reduction in activities can be observed. The HDS/HDM and the ratio of reaction between catalyst in pellet and in powder also declined. The above-mentioned formation of the external coke layer introduces an additional effect on the activity and selectivity, since the pellet/powder ratio change. In the spent catalyst, the inner reactions rate are reduced by active sites elimination (cover by coke and vanadium), and by blocking the internal pore access (ca. the loss in micro-porosity). A large part of the external layer was removed by scratching, before the powder preparation by grinding, to avoid the contamination of the internal part by the external coke layer. The micro-activity test done with D1 pellets and s-pellets under the same operating conditions demonstrates (see ratio in (1)) that s-pellets are almost 12–15% more active than pellets, confirming the role of the external coke layer in controlling the access of reactant:

$$\frac{\mathrm{HCK}_{\mathrm{D1}}^{\mathrm{pellet}}}{\mathrm{HCK}_{\mathrm{D1}}^{\mathrm{s\text{-}pellet}}} = \left[0.87\right]; \qquad \frac{\mathrm{HDS}_{\mathrm{D1}}^{\mathrm{pellet}}}{\mathrm{HDS}_{\mathrm{D1}}^{\mathrm{s\text{-}pellet}}} = \left[0.85\right];$$
$$\frac{\mathrm{HDM}_{\mathrm{D1}}^{\mathrm{pellet}}}{\mathrm{HDM}_{\mathrm{D1}}^{\mathrm{s\text{-}pellet}}} = \left[0.85\right] \tag{1}$$

Most of the effect of the carbon deposition appears early during the time on stream due to its internal and external accumulation in the particle after one week on stream. While the initial coke ages, an additional one continues to form and is deposited on top of previous one. Multi-layers of coke are formed with minimum effect on active sites elimination, but with a large contribution in closing the access to the micro- and meso-porosity. In spite of that most of the accessibly metal sites (Mo and Ni sulfide) present in meso-pores are ''auto-cleaned'' by hydrogenation of the coke precursor intermediary, and can catalyze the in-pore reactions. At high temperature, the reaction control by diffusion of resins and asphalthenes is more and more important. The external layer previously formed continues to grow by a limited sticking and reaction of insoluble material deposited during the homogeneous cracking of resins and asphalthenes. The higher the temperature, the higher the rate of thermal cracking (homogeneous) reactions and the aging of the carbonaceous layer that decrease the access to the inner structure.

3.5.3. Long run catalysts deactivation

Activity and selectivity of the samples that were on stream for six and three months at 410 and 430 °C are shown in Table 7, last two columns. All reactions are now being depleted by carbon and vanadium deposition. All the micro-porosity is lost, as well as some meso- and macro-porosity. The ratio of pellet/powder activities indicates again a lower deactivation for powder than for pellets. In addition, the micro-activity test for D4 with pellets and s-pellets (see ratios in (2)) confirms that by eliminating the external layer, between 21 and 24 % of the activities can be recovered:

$$\frac{\mathrm{HCK}_{\mathrm{D4}}^{\mathrm{pellet}}}{\mathrm{HCK}_{\mathrm{D4}}^{\mathrm{s\text{-}pellet}}} = \left[0.76\right]; \qquad \frac{\mathrm{HDS}_{\mathrm{D4}}^{\mathrm{pellet}}}{\mathrm{HDS}_{\mathrm{D4}}^{\mathrm{s\text{-}pellet}}} = [0.79];$$
$$\frac{\mathrm{HDM}_{\mathrm{D4}}^{\mathrm{pellet}}}{\mathrm{HDM}_{\mathrm{D4}}^{\mathrm{s\text{-}pellet}}} = \left[0.79\right] \tag{2}$$

The longer the time on stream, the higher is the HCK deactivation by metals and the lower is asphalthene and Conradson carbon reduction. The cracking on acid sites and the hydrogenolisis in metal site reactions have mainly been passivated by vanadium, as well as the HDM and HDS reactions that seem less affected. Two other effects occur: the addition (minor) of HDS and HDM catalytic activity by the new

Table 7
Activity and selectivity of deactivated catalyst at 410 °C, LHSV 0.5 h^{-1}

Activity/selectivity	Initial	D1	D2	D3	D4	D5
Carbon (wt%)	0	6.1	6.4	7.1	8.9	9.8
HDS/HDM activity pellet	60/53	52/48	47/44	44/42	17/21	10/5
HDS/HDM activity powder	80/67	70/62	65/59	60/57	34/27	30/24
HDS/HDM pellet selectivity	1.13	1.08	1.07	1.05	0.81	1.80
HDS/HDM powder selectivity	1.19	1.13	1.10	1.05	1.17	1.25
HDS/HDS pellet/powder	0.75	0.74	0.72	0.73	0.50	0.33
HDM/HDM pellet/powder	0.79	0.77	0.75	0.74	0.78	1.25

Ni and vanadium sulfides deposited, and the access reduction to the meso-pores where the Mo sites, which survived to the initial coke deposition, are located [9]. The higher the temperature, the worst is the latter effect.

The role of the vanadium deposited during the cycle becomes preponderant in selectivity and activity. The asphalthene micelles that were disaggregated by the temperature into small lamellas penetrated the external layer, which reacted without going further into the particle radius, and the metals were deposited as sulfide compounds in the external layer and in the meso- and macrostructure. Most of the acid sites of the catalyst disappeared early in the cycle and the primary cracking occurred by hydrogenolysis in new and old metal sites. The build up of a new layer of vanadium and nickel starts to control the access to the inner part of the pellets, and the U-shape profile of metal content as a function of particle radius develops. The low value observed for the molybdenum exposed on the surface (XPS) is probably due to the attenuation effect on the signal by the high amount of coke present nearby. The test of regenerated catalyst confirms the role of these metals in HDS and HDM. In regenerated catalyst, 40% of the meso- and 50% of the micro-porisity is recovered by removing carbon. The D4 regenerated pellet has recovered (for few hours on stream) 50% of HCK, 50% of HDS, 40% of the HDM activity as well as 40 and 34% of the asphalthene and carbon Conradson removal capabilities respect to the fresh catalyst. In regenerated catalyst, the shallow bed measurement of C_5 diffusivity, as well as the hysterisis in the nitrogen adsorption–desorption plot, indicated that pore blocking persists. All of that indicated the formation of dead end-bottle type pores by vanadium and coke:

$$\frac{\mathrm{HCK}^{\mathrm{pellet}}_{\mathrm{D4reg}}}{\mathrm{HCK}^{\mathrm{pellet}}_{\mathrm{fresh}}} = \left[0.5\right]; \qquad \frac{\mathrm{HDS}^{\mathrm{pellet}}_{\mathrm{D4reg}}}{\mathrm{HDS}^{\mathrm{pellet}}_{\mathrm{fresh}}} = \left[0.50\right];$$
$$\frac{\mathrm{HDM}^{\mathrm{pellet}}_{\mathrm{D4reg}}}{\mathrm{HDM}^{\mathrm{pellet}}_{\mathrm{fresh}}} = \left[0.40\right] \tag{3}$$

4. Conclusion

This study has demonstrated the formation and evolution of an external layer of coke in addition to the internal coke deposition in the Hydrocracking catalyst ($NiMo/Al_2O_3$) during its operation in an Ebullated bed reactor at around 50% of conversion. This external layer increased when the operating temperature was increased from 410 to 430 °C at similar HCK conversion.

The catalyst characterization indicated that the external layer that initially surrounds the catalyst is permeable and mainly composed of coke with pre-graphitic carbon structure. The micro-heterogenic-coke initially deposited inside the pellets blocks the micro-pore, reduces the meso-pore structure, and decreases all reaction rates. When the progress of the cycle, coke continues to pile up but the catalyst starts to accumulate metals and the external layer becomes less and less permeable for liquid diffusion, the activity and selectivity decrease. In addition, the diffusion of metal and sulfur containing molecules into the pores are incrementally controlled by the reduction of the interconnected cross sectional area and by pore blocking. Metals are deposited on the outer meso- and macro-pore structure, generating the typical U shape profile across the diameter of the pellets. The higher the operating temperature, the higher is the impact of the external layer closure.

Acknowledgements

The authors gratefully acknowledge the work carried out by J. Gatty and R. Patroni and to the professionals of the Analytical Laboratory, Chemistry Department, USB for the help in samples characterization.

References

[1] R. Galiasso Tailleur, T.U. Graeser, H. Herbertz, K. Nieman, H. Puxbaumer, Rev. Tecn. Intevep 2 (2) (1982) 101.
[2] T. Takatsuka, J. Chem. Eng. Japan 22 (3) (1993) 3.
[3] L. Caprioli, R. Galiasso Tailleur, M. Gutierrez, Rev. Tec. Intevep 8 (2) (1988) 115.
[4] H. Higashi, T. Takahashi, T. Kai, J. Japan Petroleum Inst. 47 (4) (2004) 297.
[5] F. Dautzemberg, J. Klunklen, 5th International Symposium Chemical Reaction Engineering Houston ACS Symposium Series, 1978, p. 65.
[6] R. Van Dongen, D. Bode, H. Van Der Eijk, J. Van Klinken, Ind. Eng. Chem. Proc. Des. Dev. 19 (1980) 630.
[7] R. Blanco, R. Galiasso Tailleur, N. Quinteros, Fuel 62 (1980) 817.
[8] J. Ancheyta, G. Betancourt, G. Centeno, G. Marroquin, Energy Fuels 17 (2) (2003) 462.
[9] M. Gray, Y. Zhao, C. McKnight, D. Komar, J.D. Carruthers, Energy Fuels 13 (5) (1999) 1037–1045.
[10] L. Caprioli, R. Galiasso Tailleur, Hydrocracking Catalyst Deactivation by Venezuelan Residue in Ebullated Bed Commercial Reactor Operation, Unpublished results, 1992.
[11] J. Wood, L.F. Gladen, Appl. Catal. A: Gen. 249 (2) (2003) 241.
[12] M.A. Callejas, M.T. Martinez, T. Blasco, W. Sastre, Appl. Catal. 218 (2001) 181.
[13] W. Sun, C. Acosta, A. Rodriguez, Ind. Eng. Chem. Res. 33 (1994) 1380–1390.
[14] J. Ramirez J., R. Galiasso Tailleur Effective diffusivity measurement in spent catalyst, Ind. Chem. Eng. Res., in preparation.
[15] D. Paerk, I.S. Do, A. Rodriguez, Catal. Rev. Sci. Eng. 38 (2) (1996) 189.
[16] L. Caprioli, R. Galiasso Tailleur, M. Gutierrez, Aiche National Meeting, Houston (TX), March 5, 1984 (paper 5f, preprint).
[17] B.G. Silbernagel, J. Catal. 56 (1979) 96.
[18] J.P. Janssens, R.M. Deugd, A.D. van Langevelt, S.T. Sie, J.A. Mujlin, in: G.F. Froment, B. Delmon, P. Grange (Eds.), Hydrotreatment and Hydrocracking of Oil Fraction, vol. 106, Elsevier, 1997, p. 283.
[19] M.T. Martinez, J.M. Jimenez, M.A. Callejas, F.J. Gomez, C. Rial, E. Carbo, in: G.F. Froment, B. Delmon, P. Grange (Eds.), Hydrotreatment and Hydrocracking of Oil Fraction, vol. 106, Elsevier, 1997, p. 311.
[20] K. Masushita, R. Koide, S. Fukase, Preprint of 220th ACS Symposium of Residuum, Washington, August 2000, p. 655.
[21] C. Philippopoulos, N. Papyannakos, Ind. Eng. Chem. Res. 27 (1988) 415.